Nuclear Medicine and Biology 43 (2016) 512–519

Contents lists available at ScienceDirect

Nuclear Medicine and Biology

journal homepage: www.elsevier.com/locate/nucmedbio

Optimization of the alkyl side chain length of fluorine-18-labeled 7α-alkyl-fluoroestradiol

Mayumi Okamoto [a,b], Hiromitsu Shibayama [c,d], Kyosuke Naka [c], Yuya Kitagawa [c], Kiichi Ishiwata [a,e,f], Isao Shimizu [c,†], Jun Toyohara [a,*]

[a] Research Team for Neuroimaging, Tokyo Metropolitan Institute of Gerontology, Tokyo, Japan
[b] Research Institute for Science and Engineering, Waseda University, Tokyo, Japan
[c] School of Advanced Science and Engineering, Waseda University, Tokyo, Japan
[d] Fine Organic Chemistry, Institute for Chemical Research, Kyoto University, Kyoto, Japan
[e] Institute for Cyclotron and Drug Discovery Research, Southern Tohoku Research Institute of Neuroscience, Koriyama, Japan
[f] Department of Biofunctional Imaging, Fukushima Medical University, Fukushima, Japan

ARTICLE INFO

Article history:
Received 14 April 2016
Received in revised form 16 May 2016
Accepted 19 May 2016

Keywords:
Estrogen receptor
C-7α-[^{18}F]FES
Structure–activity relationship
Positron emission tomography

ABSTRACT

Introduction: Several lines of evidence suggest that 7α-substituted estradiol derivatives bind to the estrogen receptor (ER). In line with this hypothesis, we designed and synthesized ^{18}F-labeled 7α-fluoroalkylestradiol (Cn-7α-[^{18}F]FES) derivatives as molecular probes for visualizing ERs. Previously, we successfully synthesized 7α-(3-[^{18}F]fluoropropyl)estradiol (C3-7α-[^{18}F]FES) and showed promising results for quantification of ER density *in vivo*, although extensive metabolism was observed in rodents. Therefore, optimization of the alkyl side chain length is needed to obtain suitable radioligands based on Cn-7α-substituted estradiol pharmacophores.

Methods: We synthesized fluoromethyl (**23**; C1-7α-[^{18}F]FES) to fluorohexyl (**26**; C6-7α-[^{18}F]FES) derivatives, except fluoropropyl (C3-7α-[^{18}F]FES) and fluoropentyl derivatives (C5-7α-[^{18}F]FES), which have been previously synthesized. *In vitro* binding to the α-subtype (ERα) isoform of ERs and *in vivo* biodistribution studies in mature female mice were carried out.

Results: The *in vitro* IC_{50} value of Cn-7α-FES tended to gradually decrease depending on the alkyl side chain length. C1-7α-[^{18}F]FES (**23**) showed the highest uptake in ER-rich tissues such as the uterus. Uterus uptake also gradually decreased depending on the alkyl side chain length. As a result, *in vivo* uterus uptake reflected the *in vitro* ERα affinity of each compound. Bone uptake, which indicates de-fluorination, was marked in 7α-(2-[^{18}F]fluoroethyl)estradiol (C2-7α-[^{18}F]FES) (**24**) and 7α-(4-[^{18}F]fluorobutyl)estradiol (C4-7α-[^{18}F]FES) (**25**) derivatives. However, C1-7α-[^{18}F]FES (**23**) and C6-7α-[^{18}F]FES (**26**) showed limited uptake in bone. As a result, *in vivo* bone uptake (de-fluorination) showed a bell-shaped pattern, depending on the alkyl side chain length. C1-7α-[^{18}F]FES (**23**) showed the same levels of uptake in uterus and bone compared with those of 16α-[^{18}F]fluoro-17β-estradiol.

Conclusions: The optimal alkyl side chain length of ^{18}F-labeled 7α-fluoroalkylestradiol was the shortest: C1-7α-[^{18}F]FES. Our results indicate that shorter chain lengths within the 4-Å ligand binding cavities of ERα are suitable for 7α-fluoroalkylestradiol derivatives.

1. Introduction

Fluorine-18-labeled steroid hormones are useful probes for positron emission tomography visualization of receptor-positive tumors such as breast and prostate cancer. Over the past 30 years, several derivatives of ^{18}F-labeled 17β-estradiol have been synthesized and evaluated. Among them, 16α-[^{18}F]fluoro-17β-estradiol (16α-[^{18}F]FES) [1] is currently used as the standard radioligand for imaging both primary and metastatic estrogen receptor-positive tumors [2,3].

On the other hand, several lines of evidence suggest that 7α-substituted estradiol derivatives bind to the estrogen receptor (ER), even though they have a long chain with complex functionality [4–11]. In contrast, small polar groups at the 7α-position do not bind well [12,13]. Furthermore, substitutions with 7α-alkyl chains bearing alcohol, carboxylic acid, and ester groups also have low affinity [6]. Thus, Anstead et al. recommended that groups at the 7α-position bind well to ERs, even if they are rather long; however, polar functions must be positioned away from the core of the steroid structure [14].

* Corresponding author at: Research Team for Neuroimaging, Tokyo Metropolitan Institute of Gerontology, 35-2 Sakae-cho, Itabashi-ku, Tokyo 173-0015, Japan. Tel.: +81 3 3964 3241; fax: +81 3 3964 1148.
E-mail address: toyohara@pet.tmig.or.jp (J. Toyohara).
† Deceased.

http://dx.doi.org/10.1016/j.nucmedbio.2016.05.008
0969-8051/

In line with this hypothesis, we are interested in the design and synthesis of 7α-fluoroalkylestradiol (Cn-7α-[^{18}F]FES) as a molecular probe to visualize ER function. Previously, French et al. synthesized the five-carbon derivative 7α-(5-[^{18}F]fluoropentyl)estradiol (C5-7α-[^{18}F]FES) and evaluated its biodistribution in immature rats [5]. Although C5-7α-[^{18}F]FES showed somewhat selective uptake in target tissues, the levels of uptake into non-target tissues were high, possibly due to the increased lipophilicity of the additional five-carbon chain. In a recent follow-up study, we investigated the shorter three-carbon derivative 7α-(3-[^{18}F]fluoropropyl)estradiol (C3-7α-[^{18}F]FES) and characterized its biological properties [15]. As expected, the shorter three-carbon chain resulted in lower uptake into non-target tissues, such as fat and blood, and the uterus-to-blood ratio at 60 min was double that of the five-carbon chain derivative. However, the three-carbon derivative underwent greater metabolic de-fluorination than the five-carbon derivative. These results indicate that opportunities still exist for further optimization of the alkyl side chain length of Cn-7α-[^{18}F]FES derivatives.

Currently, the most common route for preparing 16α-[^{18}F]FES uses 3-methoxymethyl-16β,17β-epistriol-*O*-cyclic sulfate [16]. However, some difficulties remain regarding the time required for (>30 min) acid hydrolysis of the bisulphate intermediate [17], and further optimization is required for routine clinical use in individual facilities [18]. In contrast, di-methoxymethyl-protected groups of labeling precursors of Cn-7α-[^{18}F]FES derivatives may be removed more quickly and have acceptable times required for radiosynthesis.

In this study, we further synthesized fluoromethyl (**22**; C1-7α-[^{18}F]FES) to fluorohexyl (**25**; C6-7α-[^{18}F]FES) derivatives of Cn-7α-[^{18}F]FES, except fluoropropyl (C3-7α-[^{18}F]FES) and fluoropentyl derivatives (C5-7α-[^{18}F]FES), which were synthesized previously [5,15]. We characterized the *in vitro* binding and *in vivo* distribution of these derivatives in mature female mice compared to the previously published data for C3-7α-[^{18}F]FES and 16α-[^{18}F]FES, and we discuss the optimization of the alkyl side chain length.

2. Materials and methods

2.1. Chemical synthesis

The methods of synthesis of non-radioactive compounds are outlined in Schemes 1–3, and the details are summarized in the supporting information in the online version at http://dx.doi.org/10.1016/j.nucmedbio.2016.05.008.

2.2. Radiochemical synthesis

[^{18}F]Fluoride was produced by proton irradiation of ^{18}O-enriched water (Taiyo Nippon Sanso, Tokyo, Japan) at 50 μA for 5 min using the HM-20 cyclotron (Sumitomo Heavy Industries, Tokyo, Japan). Isolation of [^{18}F]fluoride from enriched water and subsequent ^{18}F-fluorination, de-protection, purification, and formulation were carried out automatically by using a multi-purpose synthetic apparatus (MPS-200; Sumitomo Heavy Industries). Preparative high-performance liquid chromatography (HPLC) was done using a Prominence (Shimadzu, Kyoto, Japan) that was equipped with an ultraviolet (UV) absorbance detector set at 280 nm and a semiconductor radiation detector system in the indicated conditions. Radiochemical purity and specific activity (SA) of the labeled compounds were determined with the same HPLC system using the indicated conditions.

[^{18}F]Fluoride was separated with anion exchange resin (Sep-Pak Light Accell Plus QMA; Nihon Waters, Tokyo, Japan). Elution with

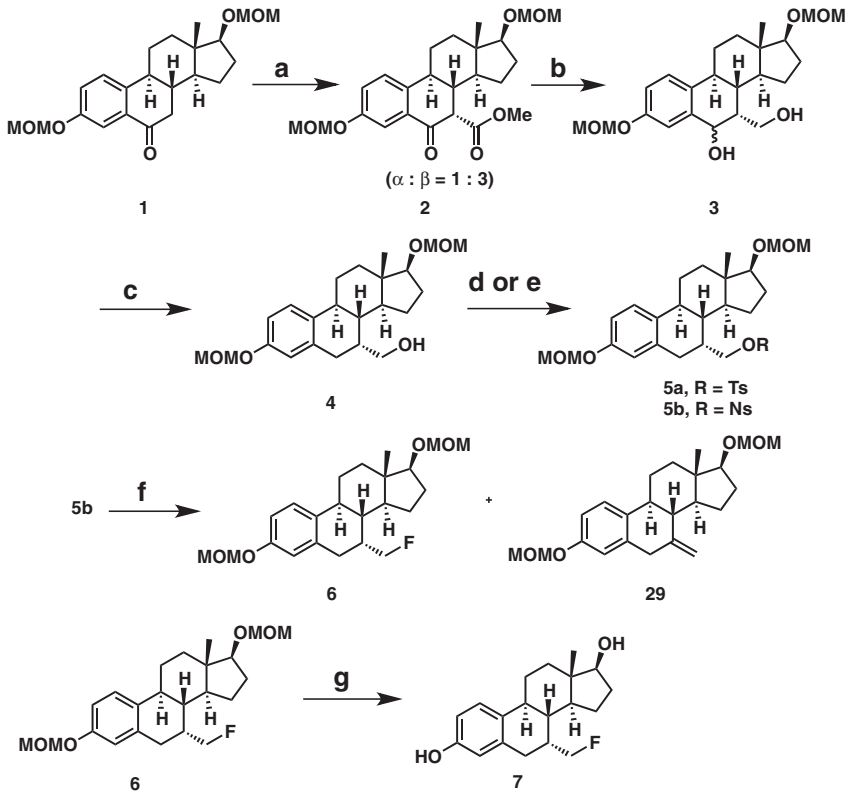

Scheme 1. Synthesis schemes for the precursor for C1-7α-[^{18}F]FES (**5a** and **5b**) synthesis and authentic standard (**7**). Reagents and conditions: (a) sodium hydride, dimethyl carbonate, reflux, 1 h (yield: 24%; α:β = 1:3); (b) lithium aluminium hydride, tetrahydrofuran, room temperature, 3 h (yield: 87%); (c) hydrogen (1 atm), palladium hydroxide, ethanol, room temperature, 6 h (yield: 73%); (d) *p*-toluenesulfonyl chloride, triethylamine, dichloromethane, room temperature, overnight (yield of **5a**: 93%), (e) *p*-nitrobenzenesulfonyl chloride, triethylamine, dichloromethane, room temperature, 2 h (yield of **5b**: 73%); (f) tetra-*n*-butyl ammonium fluoride, *tert*-butyl alcohol, reflux, 20 min (yield of **6**: 14%, yield of **29**: 22%); (g) 1 N hydrochloric acid, tetrahydrofuran, reflux, 30 min (yield: 93%).

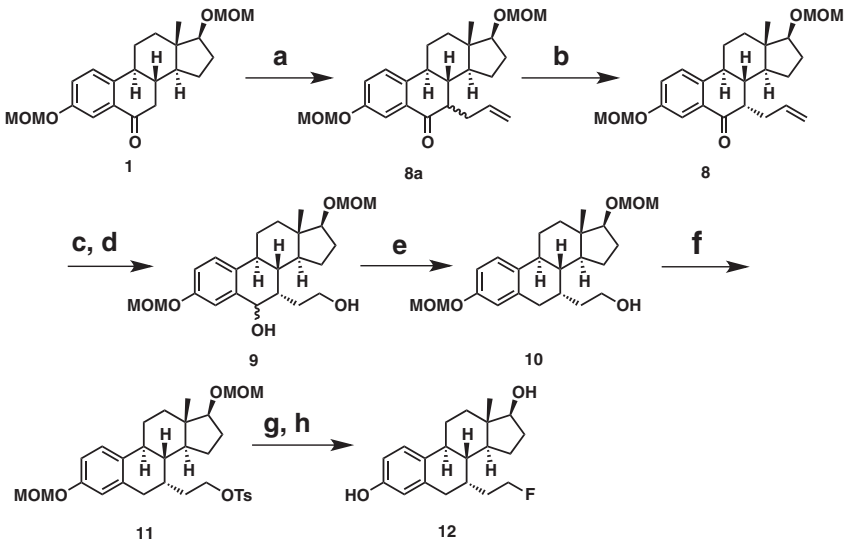

Scheme 2. Synthesis schemes for the precursor for C2-7α-[^{18}F]FES (**11**) synthesis and authentic standard (**12**). Reagents and conditions: (a) allyl iodide, potassium bis(trimethylsilyl)amide, tetrahydrofuran, 0 °C, 2 h (yield: 32%); (b) sodium methoxide, methanol, reflux, overnight (yield: quant.); (c) ozone, methanol, −78 °C, 5 min, (d) sodium borohydride, −78 °C to room temperature, overnight (yield: 78%); (e) hydrogen (1 atm), palladium hydroxide, ethanol, room temperature, 6 h (33%); (f) *p*-toluenesulfonyl chloride, triethylamine, dichloromethane, room temperature, overnight (yield: 98%); (g) tetra-*n*-butyl ammonium fluoride, acetonitrile, reflux, 15 min; (h) 1 N hydrochloric acid, reflux, 20 min (yield: 64%).

0.1 M aqueous potassium carbonate (0.3 mL, 30 μmol) resulted in a solution of potassium [^{18}F]fluoride. [^{18}F]Fluoride dissolved in 66 mmol aqueous potassium carbonate (0.3 mL, 19.8 μmol) was added to a solution of 4,7,13,16,21,24-hexaoxa-1,10-diazabicyclo[8.8.8]hexacosane (Kryptofix 222; 15 mg, 39.8 μmol; Merck Millipore, Billerica, MA) in 1 mL acetonitrile. The solvents were removed azeotropically with acetonitrile under a slight flow of helium at 100 °C. This procedure was conducted three times in total with 1.0 mL dry acetonitrile. Thereafter, 2.0 mg (3.8–4.4 μmol) each tosylate (**5a**, **11**, **21a**, and **21b**) in 1 mL dry acetonitrile was added, and the reaction mixture was heated to 100 °C

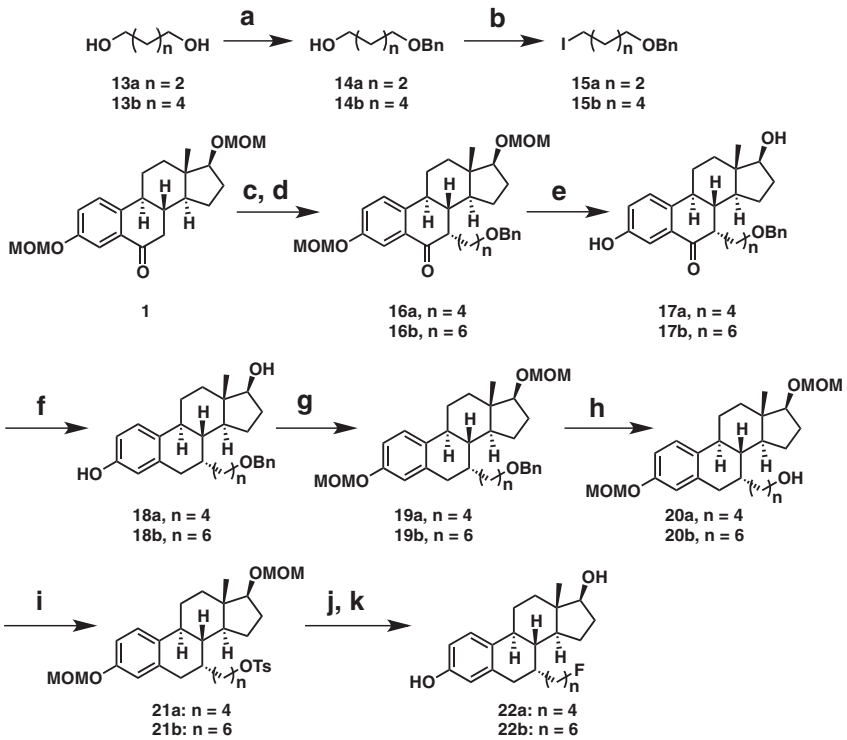

Scheme 3. Synthesis schemes for the precursor for C4- and C6-7α-[^{18}F]FES (**21a** and **21b**) synthesis and authentic standard (**22a** and **22b**). Reagents and conditions: (a) benzyl chloride, potassium hydroxide, 130 °C, 2 h (yield of **14a**: 52%, yield of **14b**: 40%); (b) triphenylphosphine, iodine, imidazole, dichloromethane, room temperature, 5 h (yield of **15a**: 73%, yield of **15b**: 88%); (c) **15a** or **16a**, potassium *tert*-butoxide, tetrahydrofuran, room temperature, overnight; (d) sodium methoxide, methanol, reflux, overnight (yield of **16a**: 40%, yield of **16b**: 56%); (e) 1 N hydrochloric acid, tetrahydrofuran, reflux, 3 h or 1 h (yield of **17a**: 74%, yield of **17b**: 84%); (f) triethylsilane, borontrifluoride–diethylether complex, dichloromethane, room temperature, overnight (yield of **18a**: 29%, yield of **18b**: 79%); (g) chloromethyl methyl ether, *N*,*N*-diisopropylethylamine, dichloromethane, reflux, overnight (yield of **19a**: 86%, yield of **19b**: 90%); (h) hydrogen (2.7 atm), palladium hydroxide, ethanol, room temperature, 2 h (yield of **20a**: 86%, yield of **20b**: 69%); (i) *p*-toluenesulfonyl chloride, triethylamine, dichloromethane, room temperature, overnight (yield of **21a**: 93%, yield of **21b**: 83%); (j) tert-*n*-butyl ammonium fluoride, acetonitrile, reflux, 20 min; (k) 1 N hydrochloric acid, reflux, 20 min (yield of **22a**: 59%, yield of **22b**: 64%).

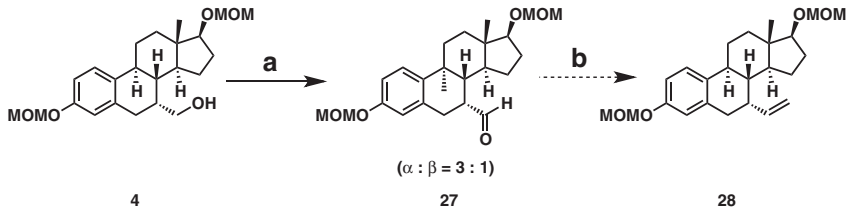

Scheme 4. Synthesis of C2-7α-alcohol (**10**) using a homologation reaction. Reagents and conditions: (a) oxalyl chloride, dimethylsulfoxide, triethylamine, dichloromethane, −78 °C, 1 h to room temperature for 20 min (α:β = 3:1); (b) triphenylphosphine, methyl iodide, *tert*-butyl alcohol, tetrahydrofuran.

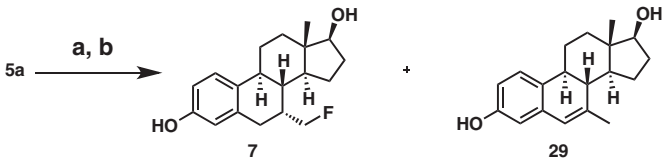

Scheme 5. Side reaction in [^{19}F]fluorination of **5a**. Reagents and conditions: (a) tert-*n*-butyl ammonium fluoride, acetonitrile, reflux, 15 min; (b) 1 N hydrochloric acid, reflux, 5 min (yield of **7**: trace, yield of **29**: 47%).

for 15 min. After removal of the solvents under a slight flow of helium at 100 °C, 0.5 N hydrochloric acid in 50% acetonitrile in water (2 mL, 1 mmol) was added, and the reaction mixture was heated to 100 °C for 2 min. The mixture was neutralized by addition of Meylon Injection 8.4% (*v*/v) (1 mL, 1 mmol; Otsuka Pharmaceutical, Naruto, Japan) and then applied to a semi-preparative HPLC column (YMC-Pack ODS-AM, 10-mm inner diameter (i.d.) × 250-mm length; YMC, Kyoto, Japan). At a 5 mL/min flow rate, a mixture of acetonitrile and water was used for the mobile phase: 45% acetonitrile in water for C1-7α-[^{18}F]FES (**23**) (t_R: 9.5 min) and C2-7α-[^{18}F]FES (**24**) (t_R: 13.1 min), and 65% acetonitrile in water for C4-7α-[^{18}F]FES (**25**) (t_R: 17.5 min) and C6-7α-[^{18}F]FES (**26**) (t_R: 20.2 min). Each [^{18}F]-product fraction was collected in a flask containing 0.1 mL of 250 mg/mL ascorbate injection (Nipro Pharma, Osaka, Japan) and evaporated to dryness. The residue was dissolved in physiological saline containing 0.125% (*v*/v) polyoxyethylene (20) sorbitan monoolate (polysorbate 80) (Wako Pure Chemical Industries, Osaka, Japan), and the solution was filtered through a 0.22-μm pore size membrane filter (Millex GV; Merck Millipore). The labeled compound was analyzed by HPLC with a YMC-Pack Pro C18 RS S-5 μm column (4.6-mm i.d. × 150-mm length; YMC) at a flow rate of 1.0 mL/min: 50% acetonitrile in water for C1-7α-[^{18}F]FES (**23**) (t_R: 2.2 min) and C4-7α-[^{18}F]FES (**25**) (t_R: 6.2 min), and 65% acetonitrile in 50 mmol sodium acetate buffer (pH 4.6) for C6-7α-[^{18}F]FES (**26**) (t_R: 4.3 min). In the case of C2-7α-[^{18}F]FES (**24**), TSKgel Super-ODS 2.3 μm (4.6-mm i.d. × 100-mm length; TOSOH, Tokyo, Japan) was used, with 45% acetonitrile in 50 mmol sodium acetate buffer (t_R: 4.1 min).

3. Biological methods

3.1. ER binding assay

[2,4,6,7-^{3}H(N)]-Estradiol ([^{3}H]estradiol; 3300 GBq/mmol, 37 MBq/mL) was purchased from PerkinElmer (Boston, MA). 16α-fluoro-17β-estradiol (16α-FES) was purchased from ABX GmbH (Radeberg, Germany). C3-7α-FES was prepared from estradiol as reported previously [15]. The purity of C3-7α-FES was confirmed by HPLC (condition 1): t_R = 18.2 min, purity = 94.5%. Human recombinant α-subtype (ERα) of the ER was purchased from Life Technologies (Carlsbad, *CA*).

Relative binding affinity (RBA) was determined by a competitive radiometric assay [15] with recombinant human ERα. Samples were incubated for 18–20 h at 4 °C, the receptor–ligand complexes were absorbed onto hydroxyapatite (Wako Pure Chemical Industries), and unbound ligand was washed away. IC_{50} values from binding displacement by blockers were determined using GraphPad Prism (GraphPad Software, San Diego, *CA*). The IC_{50} values are expressed as the mean ± standard deviation (SD) (n = 3). The binding affinities were expressed as RBA values, with the RBA of estradiol set to 100.

3.2. Biodistribution

Seven-week-old female ddY mice were purchased from Japan SLC (Hamamatsu, Japan) and allowed to acclimate for at least a week prior to use. The Animal Care and Use Committee of the Tokyo Metropolitan Institute of Gerontology approved the animal studies.

Each ^{18}F-labeled compound (0.2 MBq) was injected intravenously into mice, which were sacrificed by cervical dislocation 15 and 30 min after injection (n = 5). Blood was collected by heart puncture, and the tissues were harvested. The samples were measured for ^{18}F-radioactivity with an auto-gamma counter (1282 Commpugamma CS;

Table 1
Effect of the leaving group and solvent for fluorination of C1-7α-FES.

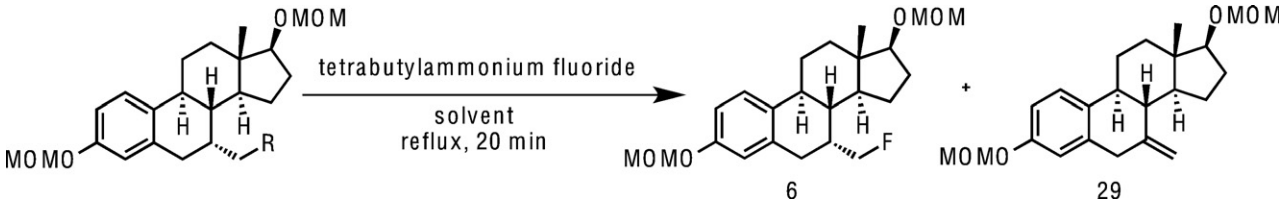

Entry	Leaving group (R)	Solvent	Yield of **6** (%)
1	tosylate	acetonitrile	trace
2	tosylate	*tert*-butyl alcohol	trace
3	nosylate	acetonitrile	trace
4	nosylate	*tert*-butyl alcohol	14 (**6**:**30** = 1:1.6)
5	nosylate	*t*-amyl alcohol	10 (**6**:**30** = 1:5.8)

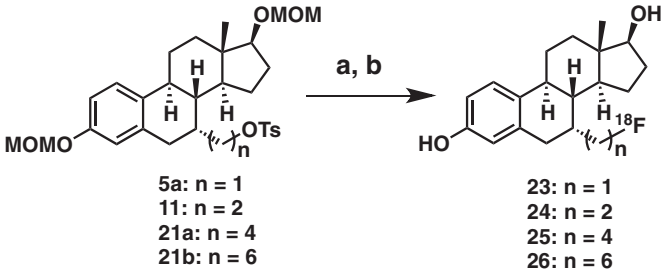

Scheme 6. Radiofluorination of Cn-7α-FES derivatives. Reagents and conditions: (a) ^{18}F-fluoride, 4,7,13,16,21,24-hexaoxa-1,10-diazabicyclo[8.8.8]hexacosane, potassium carbonate, acetonitrile, 100 °C, 15 min; (b) 0.5 N hydrochloric acid, 50% acetonitrile, 100 °C, 2 min (yield of **23**: 0.4%, yield of **24**: 9.8%, yield of **25**: 43%, yield of **26**: 44%).

LKB Wallac, Turku, Finland) and weighed. The tissue uptake of ^{18}F was expressed as dimensionless standardized uptake value (SUV) (cpm measured per gram of tissue/cpm injected per gram of body weight). The target (uterus and ovary)-to-non-target (blood and muscle) concentration ratio of radioactivity was also calculated. The previously published biodistribution data for C3-7α-[^{18}F]FES and 16α-[^{18}F]FES [15] were used for comparison with current data.

3.3. Statistical analyses

The SD of the mean was used to determine the spread of data around the mean. Differences between the tracer uptake of 16α-[^{18}F]FES and each C-7α-[^{18}F]FES derivative in organs of interest (blood, fat, ovary, uterus, and bone), the tissue-to-blood ratio (uterus-to-blood and ovary-to-blood), and the tissue-to-muscle ratio (uterus-to-muscle and ovary-to-muscle) were tested for statistical significance using one-way analysis of variance with Dunnett's multiple comparison test for independent samples. In all analyses, $P < 0.05$ was considered statistically significant. The correlation between IC_{50} and SUV was examined using Pearson's correlation coefficient. All statistical analyses were performed using GraphPad Prism (GraphPad Software, San Diego, *CA*).

4. Results and discussion

4.1. Design consideration

The first reported C5-7α-[^{18}F]FES was synthesized *via* a key reaction involving addition of a 1,6 conjugate to a dienone body using the acetyl protecting group of dihydrotestosterone as the starting material [5]. This method of synthesis cannot be universally used with other labels, and synthesis of derivatives with short side chains is particularly challenging. Therefore, we aimed to establish a novel synthesis method for Cn-7α-FES that can be used to synthesize derivatives with a variety of substituents, rather than just an ^{18}F label. First, we planned the synthesis of an ^{18}F-labeled estradiol derivative *via* an S_N2 reaction on a leaving group. We selected a nucleophilic substitution reaction with [^{18}F]fluoride, which can easily be used with the automated synthetic apparatus. Non-radioactive ^{19}F-compounds are synthesized with the same procedure. Our plan also included substitution of a side chain at Cn-7α *via* various alkylations on the C-6 ketone (**1**) and subsequent functional group replacement. We thus, selected the C-6 ketone (**1**) as the key intermediate.

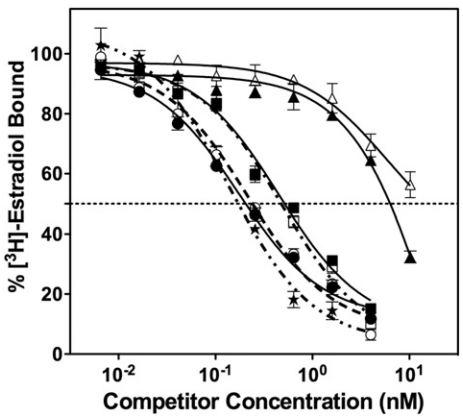

Fig. 1. Competitive binding assay of Cn-7α-FES for recombinant human ERα bound with [^{3}H]estradiol. The IC_{50} values were used to calculate relative binding affinity values (see Table 2). Solid circles = estradiol; open circles = C1-7α-FES (**7**); solid squares = C2-7α-FES (**12**); open squares = C3-7α-FES; solid triangles = C4-7α-FES (**22a**); open triangles = C6-7α-FES (**22b**); solid stars = 16α-FES. Data represent the means ± SD ($n = 3$).

4.2. Synthesis of the precursors for labeling

The key intermediate C-6 ketone (**1**) was synthesized as described previously [19]. Then, dimethyl carbonate was reacted with the C-6 ketone (**1**) in the presence of sodium hydroxide to yield β-ketoester (**2**) (Scheme 1). The synthesized β-ketoester (**2**) comprised a diastereomer mixture, with a 1:3 ratio of 7α:7β. Although 7α and 7β can be separated by column chromatography, 7α is unstable and isomerizes when incubated for several days at room temperature, resulting in a mixture containing mostly 7β. Thus, the next step should be performed immediately. The primary product during β-ketoester (**2**) synthesis was 7β, which is the stereoisomer of the desired product. However, by decarboxylation in basic conditions, we were able to recover the key intermediate C-6 ketone (**1**) from 7β at high yield. Lithium aluminium hydride reduction of β-ketoester (**2**) yielded diol **3**, after which the hydroxyl group at the benzyl-position was reduced by a hydrogenation reaction to synthesize C1-7α-alcohol (**4**) (Scheme 1).

We initially planned to synthesize the C2-7α-alcohol (**10**) using a homologation reaction based on the synthesis route of C1-7α-alcohol (**4**). However, isomerization at the C-7 position occurred *via* Swern oxidation of alcohol **4**, which resulted in a 3:1 mixture of α and β (**27**) (Scheme 4).

Thus, instead of a homologation reaction, we used an olefin synthesis route with ozone oxidation *via* an allyl body **8** with introduction of a

Table 2
Binding affinity (IC_{50} and RBA) of Cn-7α-FES derivatives and 16α-FES to the recombinant α-subtype (ERα) of the human estradiol receptor and estimated alkyl length (Å) of Cn-7α-FES derivatives.

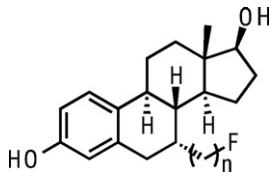

Compound	n	Estimated alkyl length (Å)	IC_{50} (nM)	RBA (%)
Estradiol			0.17 ± 0.03	100
16α-FES			0.14 ± 0.01	121
C1-7α-FES (**7**)	1	2.39	0.22 ± 0.03	77
C2-7α-FES (**11**)	2	3.78	0.45 ± 0.04	38
C3-7α-FES	3	4.99	0.47 ± 0.03	36
C4-7α-FES (**22a**)	4	6.27	5.71 ± 0.30†	3
C6-7α-FES (**22b**)	6	8.74	15.8 ± 4.18‡	1

Relative binding affinity (RBA) values of ERα in this study were determined in a competitive radiometric binding assay. Estradiol = 100%. IC_{50} data represent the mean ± SD ($n = 3$). RBA data represent the mean ($n = 3$) relative to the affinity of unlabeled estradiol as a standard.
Statistical analysis (one-way analysis of variance with Dunnett's multiple comparison test) was performed between estradiol and each Cn-7α-FES derivative and 16α-FES in IC_{50} values.
The estimated C-F alkyl chain lengths were calculated using ChemBio3D Ultra.
† $P < 0.01$ compared to estradiol.
‡ $P < 0.005$ compared to estradiol.

Table 3
Comparison of the tissue distribution of the five Cn-7α-[^{18}F]FES derivatives with 16α-[^{18}F]FES in mature female mice at 15 min post-injection.

Tissue	16α-[^{18}F]FES*	C1-7α-[^{18}F]FES	C2-7α-[^{18}F]FES	C3-7α-[^{18}F]FES*	C4-7α-[^{18}F]FES	C6-7α-[^{18}F]FES
Heart	0.22 ± 0.03	0.15 ± 0.03	0.42 ± 0.03	0.52 ± 0.04	0.64 ± 0.09	0.53 ± 0.03
Lung	0.68 ± 0.11	0.48 ± 0.06	0.76 ± 0.02	0.70 ± 0.03	0.78 ± 0.09	0.64 ± 0.11
Liver	2.77 ± 0.72	2.92 ± 0.22	2.78 ± 0.33	2.54 ± 0.16	2.55 ± 0.31	2.15 ± 0.52
Pancreas	1.36 ± 0.42	0.36 ± 0.03	0.54 ± 0.03	0.81 ± 0.15	0.58 ± 0.06	0.68 ± 0.07
Spleen	0.24 ± 0.02	0.20 ± 0.03	0.30 ± 0.01	0.32 ± 0.07	0.39 ± 0.05	0.33 ± 0.05
Small Intestine	4.02 ± 0.98	4.68 ± 1.43	2.27 ± 1.47	2.85 ± 0.57	1.21 ± 0.23	2.96 ± 0.58
Adrenal	1.82 ± 0.31	1.03 ± 0.12	1.08 ± 0.36	1.12 ± 0.19	1.17 ± 0.08	1.45 ± 0.25
Kidney	0.75 ± 0.12	0.65 ± 0.08	1.17 ± 0.64	1.06 ± 0.07	1.19 ± 0.13	0.99 ± 0.12
Muscle	0.27 ± 0.02	0.26 ± 0.03	0.29 ± 0.03	0.38 ± 0.03	0.42 ± 0.03	0.41 ± 0.05
Brain	0.19 ± 0.03	0.11 ± 0.02	0.17 ± 0.01	0.24 ± 0.03	0.33 ± 0.02	0.44 ± 0.04
Blood	0.19 ± 0.10	0.12 ± 0.03	0.51 ± 0.04§	0.49 ± 0.04§	0.68 ± 0.11§	0.32 ± 0.05†
Fat	0.62 ± 0.13	0.47 ± 0.05	0.60 ± 0.08	0.79 ± 0.14	0.57 ± 0.21	0.54 ± 0.13
Ovary	1.24 ± 0.18	1.00 ± 0.09	1.15 ± 0.37	0.89 ± 0.18†	0.80 ± 0.10‡	0.59 ± 0.16¶
Uterus	1.77 ± 0.31	1.62 ± 0.58	1.88 ± 0.74	1.36 ± 0.34	1.07 ± 0.21†	0.58 ± 0.08¶
Bone	0.28 ± 0.06	0.34 ± 0.04	1.71 ± 0.25§	1.47 ± 0.27§	1.41 ± 0.20§	0.79 ± 0.30†
Uterus/Blood	10.23 ± 3.51	14.16 ± 8.56	3.72 ± 1.58†	2.78 ± 0.66‡	1.57 ± 0.12‡	1.84 ± 0.18‡
Uterus/Muscle	6.65 ± 1.68	6.44 ± 3.22	6.60 ± 2.72	3.63 ± 1.09†	2.55 ± 0.50‡	1.41 ± 0.27¶
Ovary/Blood	7.22 ± 2.38	8.47 ± 2.69	2.25 ± 0.60¶	1.83 ± 0.41¶	1.20 ± 0.29§	1.87 ± 0.46¶
Ovary/Muscle	4.67 ± 1.03	3.89 ± 0.84	4.00 ± 1.18	2.37 ± 0.63¶	1.92 ± 0.33§	1.44 ± 0.43§

The radioactivity levels are expressed as SUV. Data represent the mean ± SD ($n = 5$).
Statistical analysis (one-way analysis of variance with Dunnett's multiple comparison test) was performed between 16α-[^{18}F]FES and each Cn-7α-[^{18}F]FES derivative in organs of interest (blood, fat, ovary, uterus, and bone), and for the tissue-to-blood ratio (uterus-to-blood and ovary-to-blood) and tissue-to-muscle ratio (uterus-to-muscle and ovary-to-muscle).
† $P < 0.05$ compared to 16α-[^{18}F]FES.
‡ $P < 0.001$ compared to 16α-[^{18}F]FES.
¶ $P < 0.0005$ compared to 16α-[^{18}F]FES.
§ $P < 0.0001$ compared to 16α-[^{18}F]FES.
* Original data expressed as % injected dose/g of 16α-[^{18}F]FES ($n = 4$) and C3-7α-[^{18}F]FES ($n = 5$) were taken from our previous report [15] and recalculated as SUV.

stereoselective side chain. An allylation reaction was performed with C-6 ketone (**1**) using allyl iodide. ^{1}H NMR demonstrated that the ratio of 7α to 7β was approximately 1:1 (**8a**). When the mixture was heated under reflux using sodium methoxide in methanol, these diastereomers isomerized to thermodynamically stable 7α (**8**) (Scheme 2). Compared to 7β, 7α with an axially bound allyl group showed greater stability; this is probably due to steric hindrance between the side chain and the CD steroid ring. Various studies on the yield from an allylation reaction were conducted regarding the type of base (potassium hexamethyldisilazane, lithium diisopropylamide), type of reaction solvent (tetrahydrofuran, 1,2-dimethoxyethane), and number of equivalents of base and allyl iodide, but the yield did not improve further. When an equivalent of base was used, the raw material remained unreacted, and when the number of equivalents of base was increased, diallyl bodies were generated (data not shown). After ozone oxidation of the terminal alkene in compound **8**, a reduction reaction was performed using sodium borohydride to yield diol **9**. The hydroxyl group at the C-6 position was then reduced by a hydrogenation reaction to yield **10** (Scheme 2). In the conversion reaction from **9** to **10**, isomerization occurred at the C-7 position, and the ratio of 7α to 7β was 6:1. We

Table 4
Comparison of the tissue distribution of the five Cn-7α-[^{18}F]FES derivatives with 16α-[^{18}F]FES in mature female mice at 30 min post-injection.

Tissue	16α-[^{18}F]FES	C1-7α-[^{18}F]FES*	C2-7α-[^{18}F]FES	C3-7α-[^{18}F]FES	C4-7α-[^{18}F]FES	C6-7α-[^{18}F]FES
Heart	0.10 ± 0.01	0.10 ± 0.04	0.23 ± 0.03	0.27 ± 0.02	0.40 ± 0.03	0.32 ± 0.04
Lung	0.30 ± 0.04	0.24 ± 0.01	0.33 ± 0.05	0.36 ± 0.03	0.48 ± 0.03	0.37 ± 0.04
Liver	1.43 ± 0.27	1.52 ± 0.16	1.13 ± 0.14	1.21 ± 0.06	1.70 ± 0.48	1.27 ± 0.22
Pancreas	0.42 ± 0.03	0.18 ± 0.02	0.26 ± 0.04	0.67 ± 0.21	0.31 ± 0.02	0.35 ± 0.05
Spleen	0.16 ± 0.01	0.11 ± 0.01	0.17 ± 0.04	0.35 ± 0.25	0.27 ± 0.02	0.23 ± 0.04
Small Intestine	3.15 ± 1.50	4.79 ± 0.91	2.17 ± 0.96	1.16 ± 0.81	1.14 ± 0.17	2.70 ± 0.76
Adrenal	0.87 ± 0.25	0.72 ± 0.33	0.52 ± 0.08	0.72 ± 0.62	0.89 ± 0.08	1.22 ± 0.23
Kidney	0.45 ± 0.08	0.43 ± 0.09	0.69 ± 0.59	0.50 ± 0.08	0.92 ± 0.41	0.61 ± 0.06
Muscle	0.19 ± 0.01	0.24 ± 0.04	0.16 ± 0.02	0.25 ± 0.04	0.28 ± 0.01	0.24 ± 0.02
Brain	0.08 ± 0.01	0.06 ± 0.00	0.10 ± 0.06	0.11 ± 0.02	0.16 ± 0.01	0.29 ± 0.03
Blood	0.14 ± 0.14	0.07 ± 0.01	0.23 ± 0.03	0.23 ± 0.02	0.43 ± 0.02§	0.19 ± 0.03
Fat	0.33 ± 0.06	0.34 ± 0.04	0.36 ± 0.07	0.51 ± 0.14	0.83 ± 0.19§	0.80 ± 0.18§
Ovary	0.99 ± 0.20	1.01 ± 0.22	0.82 ± 0.21	0.49 ± 0.20‡	0.80 ± 0.10	0.72 ± 0.07
Uterus	2.66 ± 1.09	2.44 ± 0.45	1.73 ± 0.95	1.29 ± 0.46	0.63 ± 0.15¶	0.66 ± 0.11¶
Bone	0.30 ± 0.02	0.39 ± 0.05	2.71 ± 0.70†	2.47 ± 0.75¶	2.75 ± 0.55†	0.91 ± 0.36
Uterus/Blood	31.05 ± 20.75	35.46 ± 7.75	7.36 ± 3.31‡	5.58 ± 1.94‡	1.46 ± 0.36¶	3.57 ± 1.02‡
Uterus/Muscle	13.72 ± 5.45	10.49 ± 2.68	10.11 ± 4.36	5.50 ± 2.55†	2.21 ± 0.57§	2.78 ± 0.62¶
Ovary/Blood	10.61 ± 5.30	14.83 ± 4.12	3.57 ± 0.50‡	2.14 ± 0.91‡	1.86 ± 0.26¶	3.89 ± 0.76‡
Ovary/Muscle	5.14 ± 1.41	4.27 ± 0.58	4.92 ± 0.80	2.06 ± 1.02¶	2.80 ± 0.27‡	3.04 ± 0.43‡

The radioactivity levels are expressed as SUV. Data represent the mean ± SD ($n = 5$).
Statistical analysis (one-way analysis of variance with Dunnett's multiple comparison test) was performed between 16α-[^{18}F]FES and each Cn-7α-[^{18}F]FES derivative in organs of interest (blood, fat, ovary, uterus, and bone), and for the tissue-to-blood ratio (uterus-to-blood and ovary-to-blood) and tissue-to-muscle ratio (uterus-to-muscle and ovary-to-muscle).
† P < 0.05 compared to 16α-[18F]FES.
‡ $P < 0.001$ compared to 16α-[^{18}F]FES.
¶ $P < 0.0005$ compared to 16α-[^{18}F]FES.
§ $P < 0.0001$ compared to 16α-[^{18}F]FES.
* Original data expressed as % injected dose/g of 16α-[^{18}F]FES ($n = 4$) and C3-7α-[^{18}F]FES ($n = 5$) were taken from our previous report [15] and recalculated as SUV.

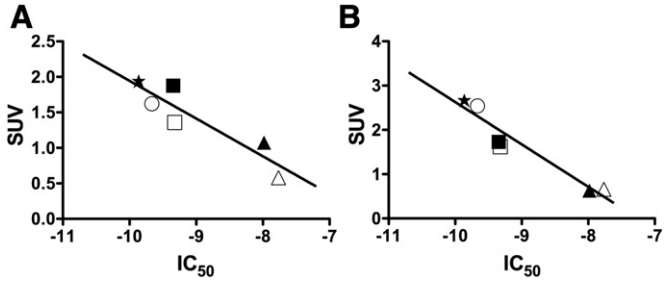

Fig. 2. Correlation between ERα affinity (IC_{50}) and uterus standardized uptake value (SUV) at 15 min (**A**) and 30 min (**B**) after injection of [^{18}F]fluoroestradiol derivatives. Open circles = C1-7α-FES (**7**); solid squares = C2-7α-FES (**12**); open squares = C3-7α-FES; solid triangles = C4-7α-FES (**22a**); open triangles = C6-7α-FES (**22b**); solid stars = 16α-FES. Data represent the means (n = 3 for IC_{50} and n = 4–5 for SUV). The correlations between IC_{50} and SUV were examined using Pearson's correlation coefficient.

believe that this was due to the production of methoxide ions in the system by sodium borohydride, resulting in a partial enolate before the C-6 position was reduced and the stereo structure of the C-7 position was broken down. However, because C2-7α-FES (eluted first) and C2-7β-FES (eluted later) could be separated by chromatography, we did not examine conditions to prevent isomerization.

Using 1,4-butanediol (**13a**) and 1,6-hexanediol (**13b**) as starting materials, the hydroxyl group on one side was protected with a benzyl group, and the other hydroxyl group was replaced with iodine by an Appel reaction, to produce side chains **15a** and **15b** (Scheme 3). Then, an alkylation reaction was performed on C-6 ketone (**1**) using **15a** and **15b** to produce **16a** and **16b**, respectively. Then, **19a** and **19b** were produced from **16a** and **16b**, respectively, in three steps. Subsequently, through a hydrogenation reaction [19], the benzyl group of the side chain was de-protected to yield alcohols **20a** and **20b**, respectively (Scheme 3).

Tosylation or nosylation of alcohols (**4**, **10**, **20a**, and **20b**) produced precursors for labeling (**5a**, **5b**, **11**, **21a**, and **21b**) (Schemes 1–3).

4.3. Examination of fluorination conditions

[^{19}F]Fluorination of tosylates (**11**, **21a**, and **21b**) using the tetra-*n*-butyl ammonium fluoride (TBAF) system in acetonitrile at reflux followed by de-protection with acid successfully produced fluorinated standards (**12**, **22a**, and **22b**). In contrast, when TBAF was reacted with tosylate **5a** under reflux in the presence of acetonitrile, the elimination reaction occurred preferentially, and the product that resulted was compound **29** as shown with ^{1}H NMR, in which olefin was isomerized by subsequent de-protection (Scheme 5).

Fluorination reactions with **5b**, in which the leaving group was converted from tosyl to nosyl, with high leaving ability were examined using a tertiary alcohol as a solvent as previously described by Kim et al. [20] (Table 1). [^{19}F]Fluorination of nosylate **5b** in *tert*-butyl alcohol improved the nucleophilic substitution reaction (**6**, 14%). After column purification of **6** and the following de-protection, **7** (93%) was produced (Scheme 1). When all steps through de-protection were performed in a single reaction, separating **7** and **29** by column chromatography was difficult. Therefore, isolation and purification were performed once after fluorination.

4.4. Radiochemical synthesis

[^{18}F]Fluorination of the tosylates was carried out using the ^{18}F-Kryptofix222-potassium carbonate system in acetonitrile at 100 °C for 15 min, followed by de-protection with 0.5 N hydrochloric acid in 50% acetonitrile at 95 °C for 5 min to yield Cn-7α-[^{18}F]FES derivatives (Scheme 6).

The desired product was purified by reversed-phase HPLC. For C2-7α-[^{18}F]FES (**24**), preparative HPLC revealed two products, corresponding to the 7α- and 7β-diastereomers. The total synthesis time was within 2 h from the end of bombardment. The decay-corrected radiochemical yields of C1-7α-[^{18}F]FES (**23**), C2-7α-[^{18}F]FES (**24**), C4-7α-[^{18}F]FES (**25**), and C6-7α-[^{18}F]FES (**26**) were 0.4%, 9.8%, 43%, and 44%, respectively. The radiochemical purity percentages of C1-7α-[^{18}F]FES (**23**), C2-7α-[^{18}F]FES (**24**), C4-7α-[^{18}F]FES (**25**), and C6-7α-[^{18}F]FES (**26**) were 98.1%, 99.2%, 100%, and 100%, respectively. Cn-7α-[^{18}F]FES derivatives showed inconspicuous UV absorbance. Calculating their SA was difficult, which may indicate a higher SA than previously reported for C3-7α-[^{18}F]FES [15]. The highest calculated SA for C3-7α-[^{18}F]FES was 55.3 GBq/μmol at the end of synthesis. Therefore, >55.3 GBq/μmol, which is equivalent to <3.6 pmol per mouse head, was used for the biodistribution study. The difference in SA between C3-7α-[^{18}F]FES and other ^{18}F-compounds may be due to the difference in the cyclotron used, the target system, irradiation conditions (current, energy, time), *etc.*

4.5. ER binding assay

The displacement curve of [^{3}H]estradiol by C1- to C3-7α-FES was parallel to the curve obtained with unlabeled estradiol, suggesting competitive binding with recombinant human ERα (Fig. 1).

C1-7α-FES (**7**) had comparable affinity as estradiol and 16α-FES for ERα (Table 2). The results also demonstrated that binding affinity to ERα increased as the carbon number decreased. The results also demonstrated that when the carbon number was ≥4, affinity dropped markedly to about 1/100 of that of estradiol.

In our present experimental conditions, the RBA values of C3-7α-FES (77%) and 16α-FES (121%) were different from those reported in

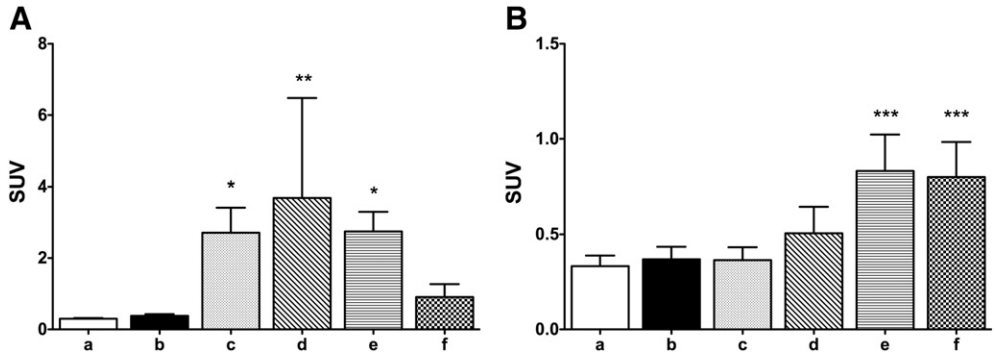

Fig. 3. Comparison of bone (**A**) and fat (**B**) uptake of [^{18}F]fluoroestradiol derivatives at 30 min post-injection. Data represent the means ± SD (n = 4–5). X-axis; a = 16α-[^{18}F]FES; b = C1-7α-[^{18}F]FES (**23**); c = C2-7α-[^{18}F]FES (**24**); d = C3-7α-[^{18}F]FES; e = C4-7α-[^{18}F]FES (**25**); f = C6-7α-[^{18}F]FES (**26**). Statistical analysis (one-way analysis of variance with Dunnett's multiple comparison test) was performed between 16α-[^{18}F]FES and each Cn-7α-[^{18}F]FES derivative. $^{*}P < 0.05$ compared to 16α-[^{18}F]FES. $^{**}P < 0.0005$ compared to 16α-[^{18}F]FES. $^{***}P < 0.0001$ compared to 16α-[^{18}F]FES. The biodistribution data for 16α-[^{18}F]FES (n = 4) and C3-7α-[^{18}F]FES (n = 5) were taken from our previous report [15] and recalculated as SUV.

previous studies: 93% and 67%, respectively [15]. These differences may be due to the different sources of recombinant ERα [21].

Some preformed pockets may be present within 4 Å at the Cn-7α-position around the ligand [22,23]. Our data suggest that when the side chain becomes longer, steric hindrance may occur. As a result, the ligand does not easily fit into the ERα pocket, and the affinity to ERα may be reduced. Furthermore, the estimated C-F alkyl chain length (Å) of Cn-7α-FES (see Table 2) strongly supports these suggestions.

4.6. Tissue distribution in normal mice

The tissue distribution data for C-7α-[^{18}F]FES (**23**, **24**, **25**, and **26**) in female mice are summarized along with previously published results (C3-7α-[^{18}F]FES and 16α-[^{18}F]FES) in Tables 3 and 4.

The uterus uptake at 30 min post-injection gradually decreased as the carbon number increased: SUV = 2.66 ± 1.09 for C1-7α-[^{18}F]FES (**23**), 1.73 ± 0.95 for C2-7α-[^{18}F]FES (**24**), 1.29 ± 0.46 for C3-7α-[^{18}F]FES, 0.63 ± 0.15 for C4-7α-[^{18}F]FES (**25**), and 0.66 ± 0.11 for C6-7α-[^{18}F]FES (**26**) (Table 4). The relationship between IC_{50} values obtained from *in vitro* ERα affinity studies and SUVs obtained from the biodistribution study is given in Fig. 2.

In vitro ERα affinity showed a significant negative correlation with the uterus uptake at 15 ($r = 0.9118$, $p = 0.0134$) and 30 min ($r = 0.9579$, $p = 0.0026$). This negative correlation was higher at 30 min than at 15 min. This phenomenon indicates that the tissue accumulation in the receptor-rich uterus may be affected by the permeability of the ligands, which is likely to be related to the relative lipophilicities.

Because radioactivity accumulation in bone reduces image contrast in positron emission tomography and is a factor that complicates image analysis, an ^{18}F label that does not readily undergo de-fluorination is desirable. As shown in Fig. 3A, radioactivity accumulation in bone at 30 min post-injection, which is thought to be due to *in vivo* metabolic de-fluorination [24], exhibited a bell-shaped curve in which C3-7α-[^{18}F]FES was at the apex and C1-7α-[^{18}F]FES (**23**) was at the lowest point. This indicates that C1-7α-[^{18}F]FES (**23**) had the highest *in vivo* ^{18}F label stability among the Cn-7α-[^{18}F]FES derivatives.

As expected, a shorter carbon chain resulted in lower uptake in fat at 30 min post-injection: SUV = 0.34 ± 0.04 for C1-7α-[^{18}F]FES (**23**), 0.36 ± 0.07 for C2-7α-[^{18}F]FES (**24**), 0.51 ± 0.14 for C3-7α-[^{18}F]FES, 0.83 ± 0.19 for C4-7α-[^{18}F]FES (**25**), and 0.80 ± 0.18 for C6-7α-[^{18}F]FES (**26**) (Fig. 3B).

5. Conclusion

In conclusion, we optimized the alkyl side chain length of Cn-7α-[^{18}F]FES derivatives. The current study revealed the impact of the alkyl side chain length of Cn-7α-[^{18}F]FES on the *in vitro* binding affinity, biodistribution, and *in vivo* metabolism. C1-7α-[^{18}F]FES (**23**) showed uterus-to-blood and ovary-to-blood ratios that were comparable to those of 16α-[^{18}F]FES. Combined with *in vivo* stability as indicated by low bone uptake and reasonably good affinity for ERα and its high target-to-non-target ratio, we suggest that C1-7α-[^{18}F]FES (**23**) is a good candidate for a novel ER probe.

Supplementary data to this article can be found online at http://dx.doi.org/10.1016/j.nucmedbio.2016.05.008.

Acknowledgments

We thank Mr. Kunpei Hayashi (SHI Accelerator Service) for his technical support with the cyclotron operation and radiosynthesis and Dr. Seijiro Hosokawa (Waseda University) and Dr. Kazuo Nagasawa (Tokyo University of Agriculture and Technology) for their valuable advice. This work was supported in part by a Grant-in Aid for Scientific Research (B) 25293271 from the Japan Society for the Promotion of Science (JSPS) and an Early Bird support project for young researchers at Waseda Research Institute for Science and Engineering.

References

[1] Kiesewetter DO, Kilbourn MR, Landvatter SW, Heiman DF, Katzenellenbogen JA, Welch MJ. Preparation of four fluorine-18-labeled estrogens and their selective uptakes in target tissues of immature rats. J Nucl Med 1984;25:1212–21.
[2] Mintun MA, Welch MJ, Siegel BA, Mathias CJ, Brodack JW, McGuire AH, et al. Breast cancer: PET imaging of estrogen receptors. Radiology 1988;169:45–8.
[3] McGuire AH, Dehdashti F, Siegel BA, Lyss AP, Brodack JW, Mathias CJ, et al. Positron tomographic assessment of 16α-[^{18}F]fluoro-17β-estradiol uptake in metastatic breast carcinoma. J Nucl Med 1991;32:1526–31.
[4] Redeuilh G, Secco C, Baulieu E-E. The use of botinyl estradiol-avidin system for the purification of "nontransformed" estrogen receptor by biohormonal affinity chromatography. J Biol Chem 1985;260:3996–4002.
[5] French AN, Wilson SR, Welch MJ, Katzenellenbogen JA. A synthesis of 7α-substituted estradiols: synthesis and biological evaluation of a 7α-pentyl-substituted BODIPY fluorescent conjugate and a fluorine-18-labeled 7α-pentylestradiol analog. Steroids 1993;58:157–69.
[6] Bucourt R, Vignau M, Torelli V, Richard-Foy H, Geynet C, Secco-Millet C, et al. New biospecific absorbents for the purification of estradiol receptor. J Biol Chem 1978;253:8221–6.
[7] Mühlenbruch B, Kirmeier F, Roth HJ. Synthesis and properties of fluorescent estradiol derivatives. Arch Pharm (Weinheim) 1986;319:196–203.
[8] Dasilva JN, van Lier JE. Synthesis and structure-affinity of a series of 7α-undecylestradiol derivatives: a potential vector for therapy and imaging of estrogen-receptor-positive cancers. J Med Chem 1990;33:430–4.
[9] Bowler J, Lilley TJ, Pittman JD, Wakeling AE. Novel steroidal pure antiestrogens. Steroids 1989;54:71–99.
[10] Weathrill PJ, Wilson APM, Nicholson RI, Davis P, Wakeling AE. Interaction of the antiestrogen ICI 164,384 with the oestrogen receptor. J Steroid Biochem 1988;30:263–6.
[11] Wakeling AE, Bowler J. ICI 182,780, a new antiestrogen with clinical potential. J Steroid Biochem 1992;43:173–7.
[12] Müller RE, Woitz HH. Post-coital contraceptive activity and estrogen receptor binding affinity of phenolic steroids. Endocrinology 1977;100:513–9.
[13] Peters RH, Crowe DF, Avery MA, Chong WKM, Tanabe M. 17-Desoxy estrogen analogues. J Med Chem 1989;32:1642–52.
[14] Anstead GM, Carlson KE, Katzenellenbogen JA. The estradiol pharmacophore: ligand structure-estrogen receptor binding affinity relationships and a model for the receptor binding site. Steroids 1997;62:268–303.
[15] Okamoto M, Naka K, Kitagawa Y, Ishiwata K, Yoshimoto M, Shimizu I, et al. Synthesis and evaluation of 7α-(3-[^{18}F]fluoropropyl) estradiol. Nucl Med Biol 2015;42:590–7.
[16] Lim JL, Zheng L, Berridge MS, Tewson TJ. The use of 3-methoxymethyl-16β,17β-epiestriol-O-cyclic sulfone as the precursor in the synthesis of F-18 16α-fluoroestradiol. Nucl Med Biol 1996;23:911–5.
[17] Kil HS, Cho HY, Lee SJ, Oh SJ, Chi DY. Alternative synthesis for the preparation of 16α-[^{18}F]fluoroestradiol. J Label Compd Radiopharm 2013;56:619–26.
[18] Zhou D, Lin M, Yasui N, Al-Qahtani MH, Dence CS, Schwarz S, et al. Optimization of the preparation of fluorine-18-labeled steroid receptor ligands 16alpha-[^{18}F]fluoroestradiol (FES), [^{18}F]fluoro furanyl norprogesterone (FFNP), and 16beta-[^{18}F]fluoro-5alpha-dihydrotestosterone (FDHT) as radiopharmaceuticals. J Label Compd Radiopharm 2014;57:371–7.
[19] Jiang XR, Sowell W, Zhu BT. Synthesis of 7α-substituted derivatives of 17β-estradiol. Steroids 2006;71:334–42.
[20] Kim DW, Jeong HJ, Lim ST, Sohn MH, Katzenellenbogen JA, Chi DY. Facile nucleophilic fluorination reactions using tert-alcohols as a reaction medium: significantly enhanced reactivity of alkali metal fluorides and improved selectivity. J Org Chem 2008;73:957–62.
[21] Freyberger A, Wilson V, Weimer M, Tan S, Tran H-S, Ahr H-J. Assessment of a robust model protocol with accelerated throughput for a human recombinant full length estrogen receptor-α binding assay: protocol optimization and intralaboratory assay performance as initial steps toward validation. Reprod Toxicol 2010;30:50–9.
[22] Katzenellenbogen JA, Muthyala R, Katzenellenbogen BS. The nature of the ligand-binding pocket of estrogen receptor α and β: the search for subtype-selective ligands and implications for the prediction of estrogenic activity. Pure Appl Chem 2003;75:2397–403.
[23] Minutolo F, Macchia M, Katzenellenbogen BS, Katzenellenbogen JA. Estrogen receptor β ligands: recent advances and biomedical applications. Med Res Rev 2011;31:364–442.
[24] Fiserova-Bergerova V. Changes of fluoride content in bone: an index of drug defluorination in vivo. Anesthesiology 1973;38:345–51.